



# Suppressing Efficiency Roll-Off of TADF Based OLEDs by Constructing Emitting Layer With Dual Delayed Fluorescence

Yuewei Zhang<sup>1</sup>, Zhiqiang Li<sup>1</sup>, Chenglong Li<sup>1,2\*</sup> and Yue Wang<sup>1\*</sup>

<sup>1</sup> State Key Laboratory of Supramolecular Structure and Materials, Jilin University, Changchun, China, <sup>2</sup> State Key Laboratory on Integrated Optoelectronics, Key Laboratory of Advanced Gas Sensors, College of Electronic Science and Engineering, Jilin University, Changchun, China

To suppress efficiency roll-off induced by triplet-triplet annihilation (TTA) and singlet-triplet annihilation (STA) in thermally activated delayed fluorescence (TADF) based organic light emitting diodes (OLEDs) is still a challenge. This issue was efficiently addressed by generating dual delayed fluorescence in the emitting layer of OLEDs. A novel TADF compound, PXZ-CMO, featuring a D-A structure was designed and synthesized. By dispersing the emitter into different hosts, devices G1 (MCP host) and G2 (DPEPO host) with identical configurations were carefully fabricated, which showed similar maximum EQE/CE of 12.1%/38.2 cd A<sup>-1</sup> and 11.8%/33.1 cd A<sup>-1</sup>, respectively. Despite severe efficiency roll-off in device G2 with only 6.4% EQE remaining at a luminance of 1,000 cd m<sup>-2</sup>, a remarkably reduced efficiency roll-off was attained in device G1, retaining EQE as high as 10.4% at the same luminance of 1,000 cd m<sup>-2</sup>. The excellent device performance with reduced roll-off in device G1 should result from the dual delayed fluorescence in the emitting layer, which possesses great advantages in achieving dynamic and adaptive exciton distribution for radiation acceleration and quench suppression.

**Keywords:** thermally activated delayed fluorescence, organic light emitting diodes, dual delayed fluorescence, efficiency roll-off, donor-acceptor

## OPEN ACCESS

### Edited by:

Lian Duan,  
Tsinghua University, China

### Reviewed by:

Zuo-Quan Jiang,  
Soochow University, China  
Albert Moyano,  
University of Barcelona, Spain

### \*Correspondence:

Chenglong Li  
chenglongli@jlu.edu.cn  
Yue Wang  
yuewang@jlu.edu.cn

### Specialty section:

This article was submitted to  
Organic Chemistry,  
a section of the journal  
Frontiers in Chemistry

Received: 27 January 2019

Accepted: 15 April 2019

Published: 30 April 2019

### Citation:

Zhang Y, Li Z, Li C and Wang Y (2019)  
Suppressing Efficiency Roll-Off of  
TADF Based OLEDs by Constructing  
Emitting Layer With Dual Delayed  
Fluorescence. *Front. Chem.* 7:302.  
doi: 10.3389/fchem.2019.00302

## INTRODUCTION

Recently, thermally activated delayed fluorescence (TADF) materials based on pure organic aromatic molecules have drawn great attention for their nature to achieve 100% exciton utilization in organic light emitting diodes (OLEDs) (Uoyama et al., 2012; Tao et al., 2014; Zhang et al., 2014a; Kaji et al., 2015; Liu et al., 2015, 2017; Cho et al., 2016; Data et al., 2016; Li et al., 2016; Chen et al., 2017). TADF-OLEDs with high external quantum efficiencies (EQEs) of over 20% have been reported within the visible light spectrum region. However, they still suffer from severe efficiency roll-offs and often exhibited quite low EQEs at a brightness of over 1,000 cd m<sup>-2</sup>, which is the required value for the practical application (Wang et al., 2014; Lin et al., 2016; Rajamalli et al., 2016; Huang et al., 2017; Wu et al., 2018; Zeng et al., 2018). For most of TADF emitters this is a great issue, which can induce the increase of power consumption, reduction of device lifetime, and limitation of their extensive applications. For TADF-OLEDs, the electrically generated triplet excitons contribute to emission through reverse intersystem crossing (RISC) process (Figure 1A), which can result in the transformation from triplet (T<sub>1</sub>) to singlet (S<sub>1</sub>) and sequential single excited state radiation transition.

To accomplish the RISC process, a relatively long time is essential. Therefore, in emitting layer (EML), the accumulation of  $T_1$  excitons is unavoidable, leading to intense  $T_1$ - $T_1$  annihilation (TTA), and  $S_1$ - $T_1$  annihilation (STA). The TTA and STA can result in remarkable efficiency roll-off. In principle, the efficiency roll-off can be suppressed by reducing delayed lifetime and concentration of  $T_1$  excitons. It was demonstrated that the TADF emitters with shorter delayed lifetimes displayed relatively smaller efficiency roll-offs (Numata et al., 2015; Lee et al., 2016, 2017). On the other hand, to promote both of phosphorescence and delayed fluorescence in OLEDs could also suppress the efficiency roll-off (Zhang et al., 2016a; Wei et al., 2017; Yu et al., 2017). To dilute the  $T_1$  excitons within an EML, a scheme for establishing the single molecule based dual- or multi- $T_1$  excited states with different lifetimes and similar emission maxima was proposed (Figure 1B). It is rational to expect a breakthrough in EL performance based on this dual delayed fluorescence mechanism from both  $S_1$  and  $T_1$  states, which theoretically possesses great advantages in achieving dynamic and adaptive exciton distribution for radiation acceleration and quench suppression. However, so far, the construction of TADF systems with dual- or multi- $T_1$  excited states still remains a great challenge.

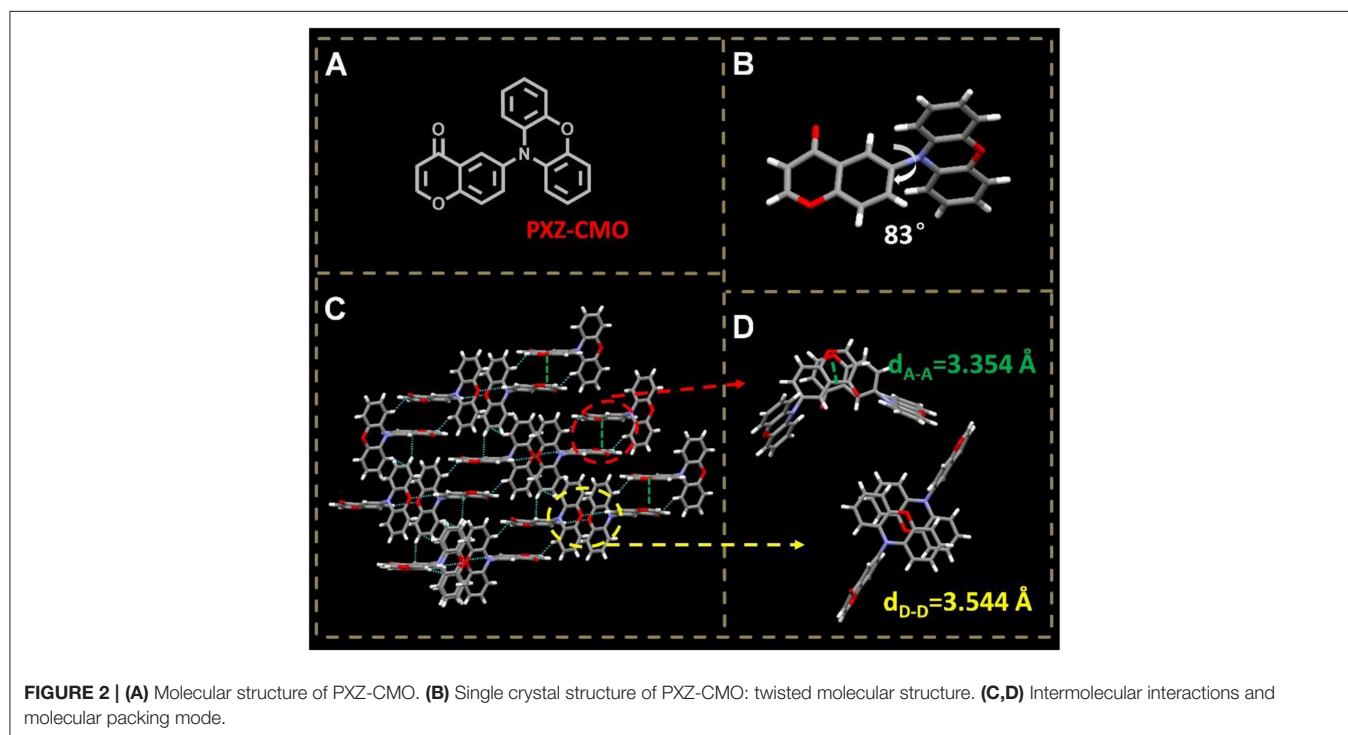
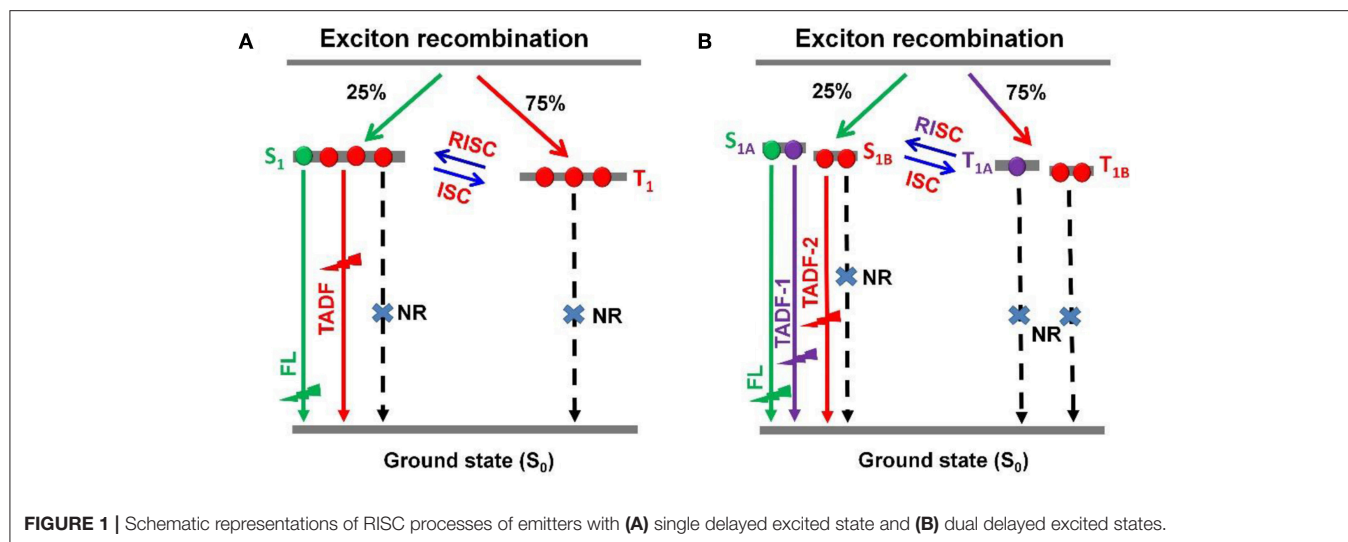
To achieve TADF, the excited states generally have intramolecular-charge-transfer (ICT) characteristic and the molecules are composed of spatially separated donor (D) and acceptor (A) moieties. Upon transformation from ground state to excited state, the molecules undergo internal electron transfer from D to A, which is usually accompanied by molecular conformation change resulting a new dipolar state to stabilize the excited state. It was demonstrated that the above process could be dominated by the environment polarity when the TADF molecules were doped in some matrixes (Grabowski et al., 2003; Aydemir et al., 2015, 2017; Data et al., 2016). Upon a kind of TADF molecules are doped into a host, the molecules may exist under different polarity and rigidity circumstances, which can induce different excited states. Additionally, the D-A type molecules containing pseudo-planar fragments, such as xanthone (XO), 9,9-dimethyl-9,10-dihydroacridine (DMAC), and phenoxazine (PXZ), have the potential to adopt different molecular configurations (Zhang et al., 2016b, 2017; Wang et al., 2017). Therefore, by dispersing the emitters in suitable hosts with distinct polarity and steric hindrance, dual- or multi- $T_1$  excited states may be generated from one kind of TADF molecules (Méhés et al., 2014; Zhang et al., 2014b). To evaluate our hypothesis, 4H-chromen-4-one (CMO) and phenoxazine (PXZ) were selected as the electron A and D moieties, respectively, to construct a target TADF molecule PXZ-CMO (Figure 2A). 1,3-bis(carbazol-9-yl)benzene (MCP) with weak polarity and bis(2-(diphenylphosphino)phenyl)ether oxide (DPEPO) with strong polarity were employed as the hosts to prepare the emitting layer of OLEDs, respectively (Lee et al., 2014). In this contribution, we successfully develop an effective strategy to reduce the efficiency roll-off of TADF-OLEDs based on the dual delayed fluorescence in the emitting layer.

## RESULTS AND DISCUSSION

### Synthesis, Crystal and Photophysical Properties

A TADF emitter 6-(10H-phenoxazin-10-yl)-4H-chromen-4-one, namely PXZ-CMO, was synthesized via Buchwald-Hartwig cross coupling between 6-bromo-4H-chromen-4-one and PXZ with high yields (Scheme S1) (Wolfe et al., 1998; Littke et al., 2002; Hooper et al., 2003; Fu, 2008). The single-crystal X-ray diffraction analyses demonstrated that both the PXZ and CMO moieties adopt perfect planar  $\pi$ -conjugated structure feature. The D and A planes are linked together by a single bond, which is beneficial to the regulation of molecular conformation. The crystal is generated based on moderate intermolecular  $\pi\cdots\pi$  stacking interactions (acceptor $\cdots$ acceptor contacts) accompanied by noncovalent bonds such as C-H $\cdots$ O, O=C $\cdots$ H-C, and C-H $\cdots\pi$  interactions (Figures 2C,D), which can enhance the charge transfer ability (Wang et al., 2013). Since the highly twisted structure with large dihedral angle of  $83^\circ$  between D and A planes, the highest occupied molecular orbital (HOMO) and the lowest unoccupied molecular orbital (LUMO) of PXZ-CMO are mainly localized on the D and A moieties (Figure 2B and Figure S1), respectively. Therefore, the energy gap ( $\Delta E_{ST}$ ) between the lowest singlet excited state ( $S_1$ ) and triplet excited state ( $T_1$ ) is as small as 0.02 eV, which was calculated based on spectroscopic data in Figure S2. Obviously, the  $\Delta E_{ST}$  value is small enough to promote the reverse intersystem crossing (RISC) from  $T_1$  to  $S_1$  (Yang et al., 2017).

The UV-vis absorption and emission spectra of PXZ-CMO in various solvents with different polarity were shown in Figure S3 and the photophysical data were summarized in Table S1. The strong absorption band at around 310 nm can be attributed to the  $\pi$ - $\pi^*$  transition of the PXZ, and the other weak and broad absorption band at longer wavelengths from 345 to 420 nm can be assigned to the ICT absorption from D (PXZ) to A (CMO). PXZ-CMO emission spectra displayed a significant solvatochromic phenomenon and the emission maxima displayed red-shift from 398 nm in toluene to 524 nm in dichloromethane. The largely solvatochromic red-shift indicated a typical ICT feature of PXZ-CMO, suggesting a large change of dipole moment in the electronically excited state (Guo et al., 2014; Wang et al., 2015; Li et al., 2017). Moreover, emissions that originated from local excited (LE) states could also be observed in toluene and THF solutions, which further demonstrated a weak electronic coupling between PXZ and CMO units. The transient PL decays for PXZ-CMO were measured in dilute solutions under nitrogen atmosphere (Figure S4). Unlike the behavior of conventional TADF molecules, its long-lived TADF emission was completely quenched by non-radiative decay in solution and only the prompt components with nanosecond-scale lifetimes were observed (Zhang et al., 2012, 2014c). In solid state, PXZ-CMO displayed a prompt lifetime of 93 ns and a delayed lifetime of 1.6  $\mu$ s (Figure S5). The PXZ-CMO solid exhibited photoluminescence quantum yield (PLQY) of 27.6% and emission maximum of 518 nm (Table S1 and Figure S6). Thermogravimetric analysis (TGA) and differential scanning calorimetry (DSC) measurements revealed that PXZ-CMO

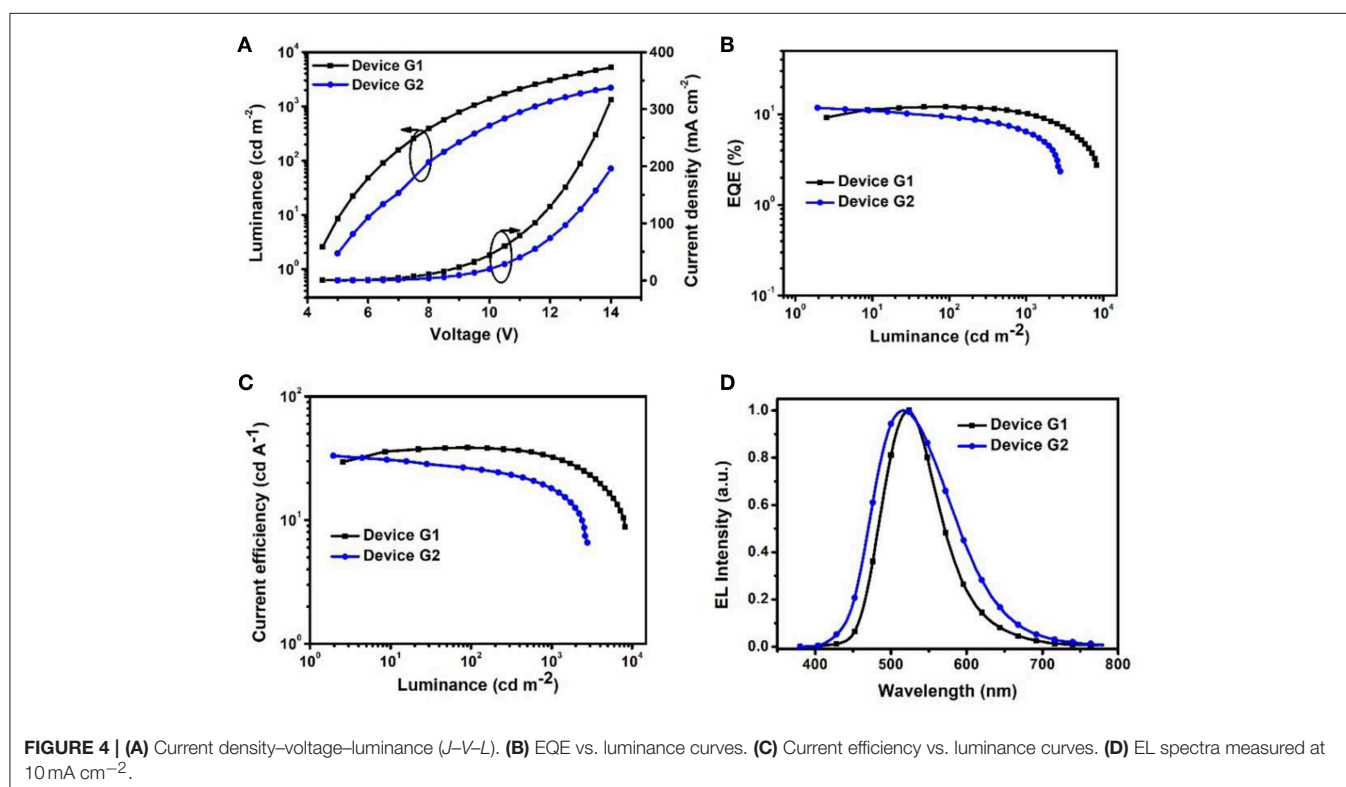
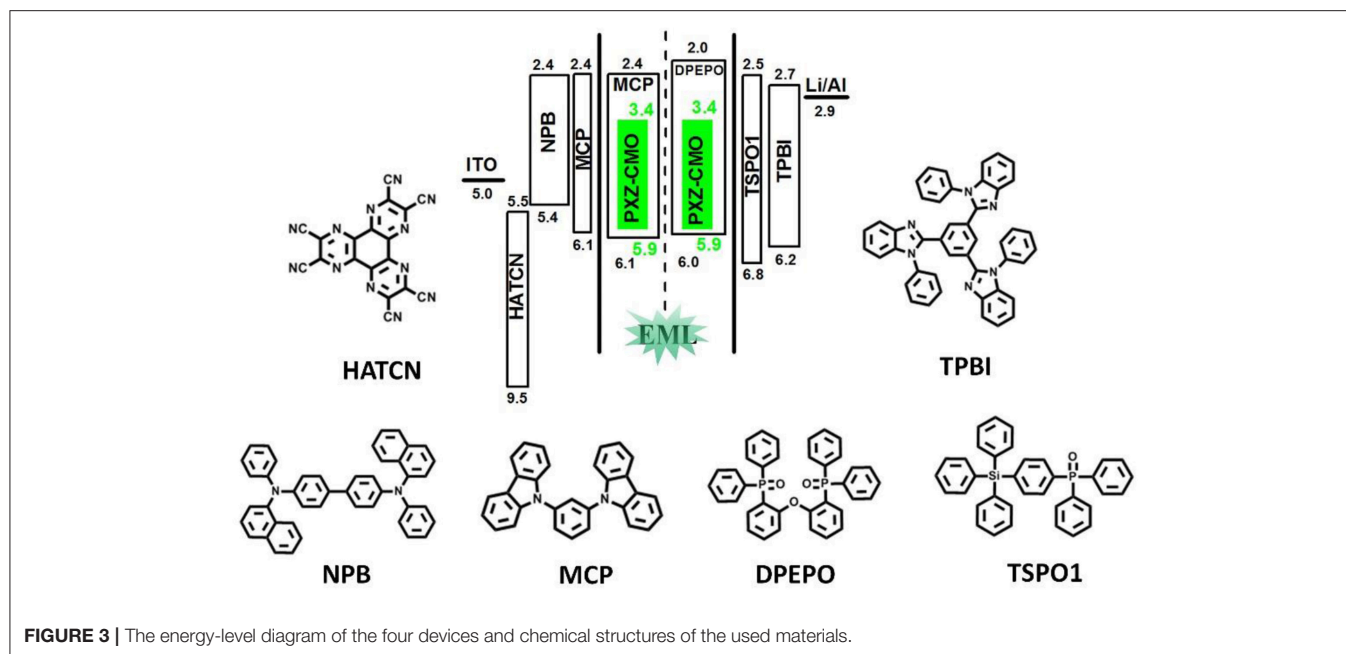


possessed a good thermal stability with a thermal decomposition temperature ( $T_{d5}$ , corresponding to 5% weight loss) of  $261^{\circ}\text{C}$  and a melting point ( $T_m$ ) of  $187^{\circ}\text{C}$  (Figure S7). The HOMO ( $-5.95\text{ eV}$ ) and LUMO ( $-3.35\text{ eV}$ ) energy levels of PXZ-CMO were obtained from the onsets of the oxidation and reduction curves (Figure S8).

### Electroluminescence Performance

To evaluate the electroluminescent (EL) performance of PXZ-CMO, we fabricated multi-layer OLEDs with a structure of [ITO/HATCN (5 nm)/NPB (60 nm)/MCP (5 nm)/EML (30 nm)/TSPO1 (5 nm)/TPBi (30 nm)/LiF (0.5 nm)/Al (150 nm)]

(Figure 3). ITO (indium-tin oxide) and LiF/Al (lithium fluoride/aluminum) were used as anode and cathode, respectively. HATCN (1,4,5,8,9,11-hexaazatriphenylene hexacarbonitrile), NPB (1,4-bis[(1-naphthylphenyl)amino]biphenyl), and TPBi (1,3,5-tris[(N-phenylbenzimidazol-2-yl)benzene]) were selected as hole-injection (HIL), hole-transporting (HTL) and electron-transporting layers (ETL), respectively. MCP ( $T_1 = 2.90\text{ eV}$ ) and TSPO1 (diphenyl-4-triphenylsilylphenyl-phosphine oxide with high  $T_1$  ( $3.36\text{ eV}$ )) were acted as the exciton-blocking layers (Kim and Lee, 2014). The doped thin films of PXZ-MCO (dopant) in solid hosts of MCP or DPEPO ( $T_1 = 3.10\text{ eV}$ ) with different dopant

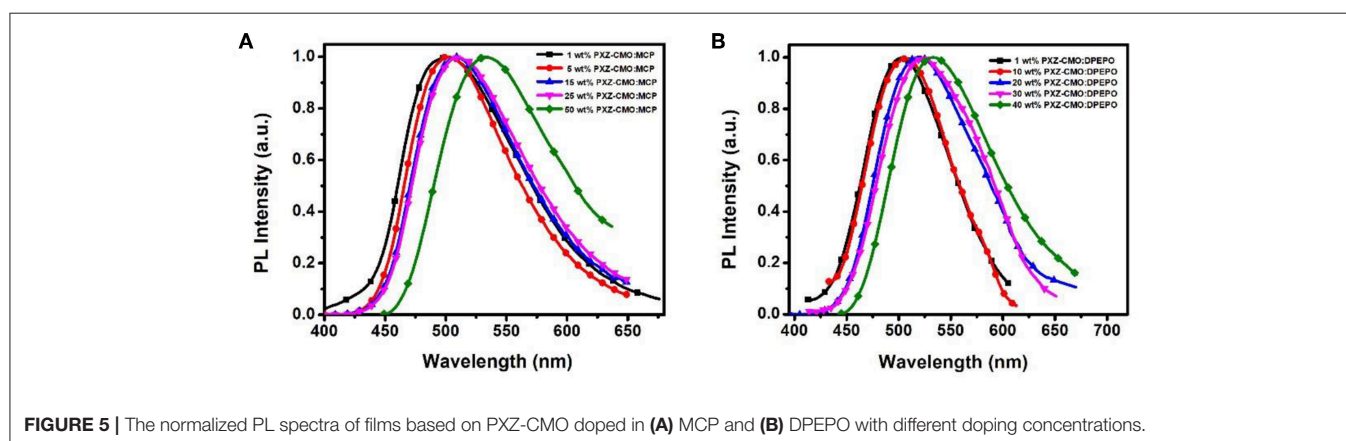


concentrations from 5 to 30 wt% were employed as the emitting layers (EMLs). **Table 1** presents the key EL parameters of PXZ-CMO based OLEDs with various dopant concentrations (5, 15, 25 wt% PXZ-CMO doped in MCP and 10, 15, 20, 30 wt% PXZ-CMO doped in DPEPO). Obviously, the DPEPO-based devices all showed more severe efficiency roll-offs than that of the MCP-based ones. When 15 and 20 wt% dopant

concentrations were employed, the MCP- and DPEPO-based devices displayed the best performances with the highest external quantum efficiencies (EQEs) of 12.1 and 11.8%, respectively. The photoluminescence quantum yields (PLQYs) of film A (15 wt% PXZ-CMO:MCP) and film B (20 wt% PXZ-CMO:DPEPO) were 48.7% and 35.0% (**Table S1**), respectively. Thus, almost all  $T_1$  excitons were up-converted into  $S_1$  excitons and utilized

**TABLE 1** | Summary of the EL data of OLEDs based on PXZ-CMO doped in MCP/DPEPO with different doping concentrations.

Device	$V_{\text{turn-on}}$ (V) <sup>a</sup>	$L_{\text{max}}$ /cd m <sup>-2</sup> (V at $L_{\text{max}}$ )	$CE^b$ /cd A <sup>-1</sup>	$EQE^b$ /%	Roll-offs <sup>c</sup> /%	EL $\lambda_{\text{max}}$ /nm, CIE (x, y) <sup>d</sup>
5 wt% PXZ-CMO:MCP	4.0	6,968 (16.5)	28.63/24.13	10.20/10.20/8.40	17.65	504 (0.26, 0.51)
15 wt% PXZ-CMO:MCP	4.5	8,214 (16.5)	38.20/32.70	12.10/12.10/10.40	10.05	524 (0.28, 0.55)
25 wt% PXZ-CMO:MCP	5.0	7,475 (16.0)	29.90/27.71	9.79/9.75/9.10	7.05	516 (0.29, 0.56)
10 wt% PXZ-CMO:DPEPO	5.0	2,606 (15.0)	27.48/17.78	10.37/8.20/5.87	43.39	524 (0.28, 0.54)
15 wt% PXZ-CMO:DPEPO	4.9	2,685 (15.0)	29.04/15.12	10.77/9.20/5.37	50.14	516 (0.31, 0.48)
20 wt% PXZ-CMO:DPEPO	5.0	2,780 (16.0)	33.10/18.10	11.80/6.40	45.76	517 (0.30, 0.48)
30 wt% PXZ-CMO:DPEPO	5.1	2,494 (16.0)	32.42/17.95	11.43/6.33	44.62	516 (0.30, 0.48)

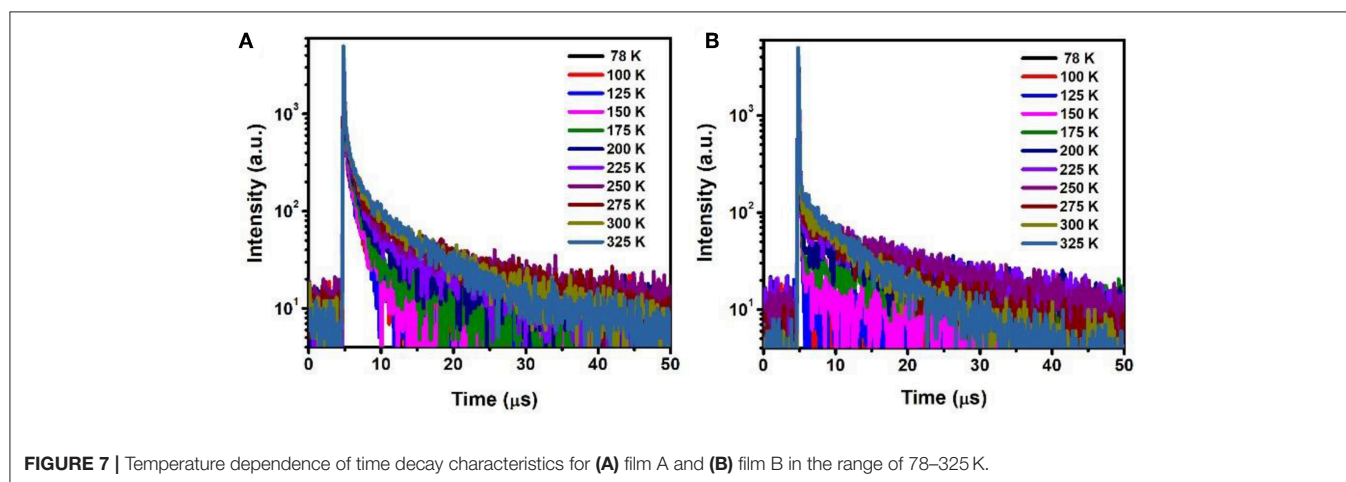
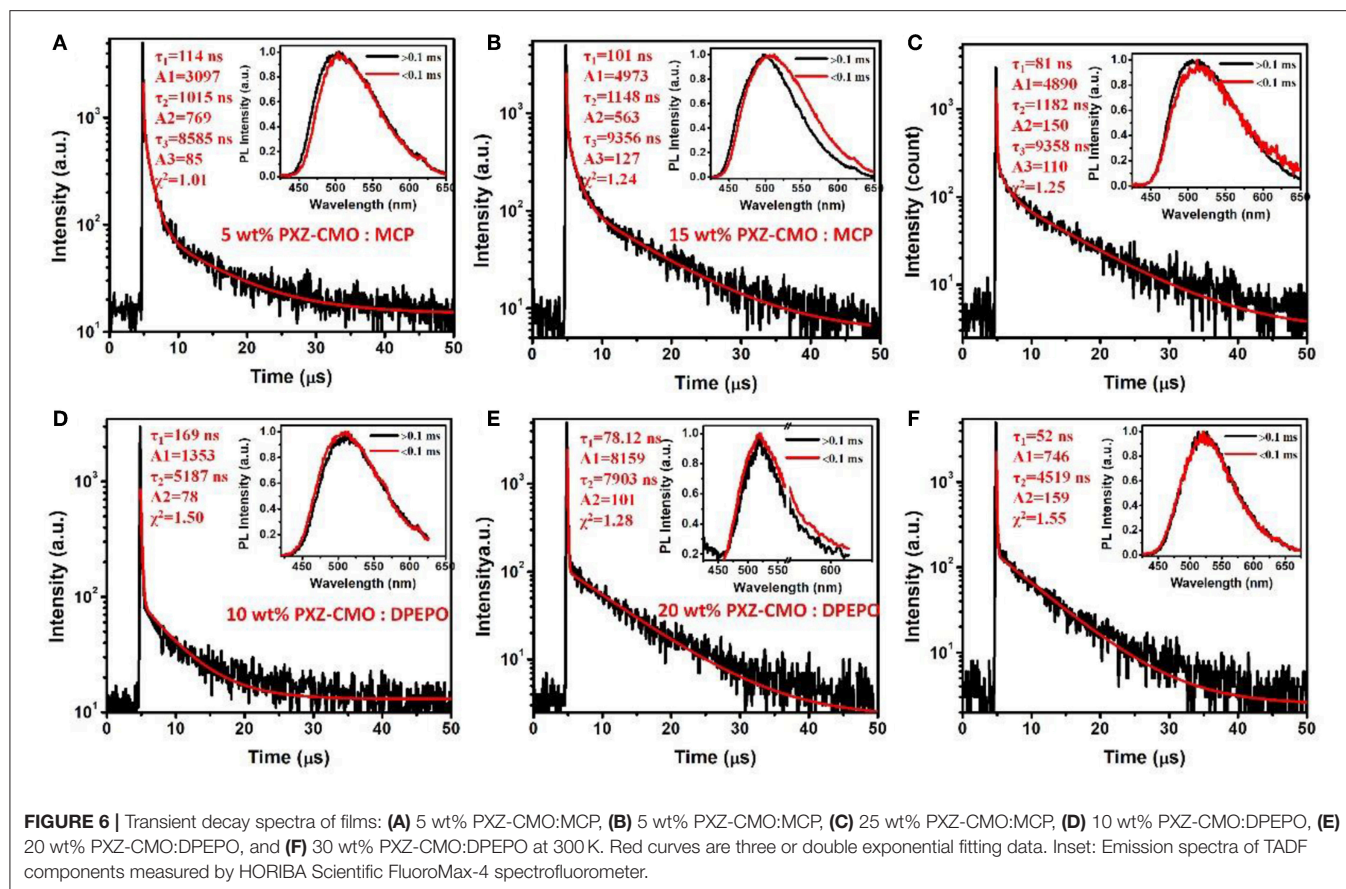
<sup>a</sup>Obtained at 1 cd m<sup>-2</sup>.<sup>b</sup>Maximum efficiencies/efficiencies at 100 cd m<sup>-2</sup>/efficiencies at 1,000 cd m<sup>-2</sup>.<sup>c</sup>EQE roll-offs at 1,000 cd m<sup>-2</sup>.<sup>d</sup>Recorded at 10 mA cm<sup>-2</sup>.**FIGURE 5** | The normalized PL spectra of films based on PXZ-CMO doped in (A) MCP and (B) DPEPO with different doping concentrations.

for electroluminescence, resulting in high EQEs. The finally optimized EMLs are 15 wt% PXZ-CMO:MCP (Device G1) and 20 wt% PXZ-CMO:DPEPO (Device G2). The current density–voltage–luminance ( $J$ - $V$ - $L$ ), EQE–luminance ( $EQE$ - $L$ ), current efficiency–luminance ( $CE$ - $L$ ) characteristics, and EL spectra of devices G1 and G2 were presented in **Figure 4**. Devices G1 and G2 exhibited emission maxima at 524 and 517 nm with corresponding Commission Internationale de l’Eclairage (CIE) color coordinates of (0.28, 0.55) and (0.30, 0.48), respectively (**Figure 3D**). Additionally, the EL spectra demonstrated negligible change with increasing driving voltages (**Figure S9**). Devices G1 and G2 showed comparable highest EQE values, however, the efficiency roll-off of device G1 was remarkably small compared with that of device G2. Under a high luminance of 1,000 cd m<sup>-2</sup>, G1 maintained its EQE at 10.4%, while the EQE of G2 reduced to 6.4%.

## Carrier Transport and Transient PL Spectra Properties

Firstly, we evaluate the carrier transport properties of PXZ-CMO doped in MCP and DPEPO. The single-carrier devices with the structures of [ITO/NPB (10 nm)/15% PXZ-CMO:MCP or 20% PXZ-CMO:DPEPO (80 nm)/NPB (10 nm)/Al (100 nm)] for the hole-only device and [ITO/TPBI (10 nm)/15% PXZ-CMO:MCP or 20% PXZ-CMO:DPEPO (80 nm)/TPBI (10 nm)/LiF (1 nm)/Al

(100 nm)] for the electron-only device were fabricated. The NPB and TPBI layers are used to prevent the electron and hole injection from the cathode and anode, respectively. As depicted in **Figure S10**, both hole and electron current density of 15% PXZ-CMO:MCP are higher than that of 20% PXZ-CMO:DPEPO at the same driving voltage, suggesting better ability for conducting both electrons and holes. However, both two doped films exhibit balanced carrier transport property, indicating that the different efficiency roll-off behaviors of devices G1 and G2 should not be attributed to be the difference of the carrier transport. To further understand the reasons of the different efficiency roll-off behaviors of devices G1 and G2, detail photophysical investigations of PXZ-CMO:MCP and PXZ-CMO:DPEPO doped films were performed and detailed data were summarized in **Table S2**. As shown in **Figures 5, 6**, the delayed PL emissions all presented similar spectral distributions as that of the prompt PL emissions, implying that the delayed and prompt fluorescence of these films originated from the same emissive singlet states (Kim et al., 2018). Upon fitting the transient PL decays of PXZ-CMO:MCP doped films, a clear third-order exponential decay could be found, revealing the presence of two delayed fluorescence processes with characteristic time constants of around 1.1 and 9.1  $\mu$ s, respectively. Moreover, for PXZ-CMO:MCP films, the integral ration of the relatively shorter delayed lifetime



remarkably decreased and the longer delayed lifetime showed a reverse tendency with increasing the doped concentration. While the PXZ-CMO:DPEPO doped films showed only one delayed lifetime (around 6.5  $\mu$ s), testifying the typical TADF feature with a single delayed fluorescence process. In films with the doped concentration of over 5 wt%, the PXZ-CMO molecules should not adopt mono-dispersed state and assemble into small aggregates, which could be proved by the obvious spectral redshift of the green emission in both MCP- and DPEPO-based

films as the doping concentration is increased (**Figure 5**). Since MCP is a weakly polar host, DPEPO is a strongly polar host, and the polarity of PXZ-CMO molecule with D-A structural feature is also very strong. Therefore, from the perspective of polarity, PXZ-CMO and DPEPO are similar with each other, while PXZ-CMO and MCP are different. For the PXZ-CMO aggregates within MCP matrix, the PXZ-CMO molecules should be in strong polarity environment (the inside of aggregates) or weak polarity environment (the surface of aggregates). The

different polarity environment can not only induce different excited state characteristics (two kinds of delayed lifetimes in MCP-based films), but also increase the distance between these two  $T_1$  states to prevent the TTA process, which occurs by a diffusion-limited, short-range electron exchange process (Dexter mechanism) (O'Brien et al., 2009). Differently, in PXZ-CMO:DPEPO doped films, both the dopant and host molecules possess strong polarity, therefore only one delayed lifetime was observed, similar to the PXZ-CMO solids. In addition, the singlet CT state in a polar matrix of DPEPO will be more stabilized than that of MCP, resulting in a theoretically smaller  $\Delta E_{ST}$  values as well as faster RISC rates (shorter TADF lifetimes) in DPEPO-based films. However, according to the formula  $\tau_{av} = \sum A_i \tau_i^2 / \sum A_i \tau_i$  (Zhang et al., 2014c), the average lifetime of film A (6.5  $\mu$ s) is actually similar to that of PXZ-CMO:DPEPO doped films (5.2–7.9  $\mu$ s) at 300 K. This phenomenon indicates that not only the polarity of the host but also some potential interactions (such as  $\pi$ - $\pi$  interactions) between the emitter and the host affect the RISC rate (Cai et al., 2017), because MCP has the potential  $\pi$ - $\pi$  interaction groups of carbazole, while DPEPO doesn't. Thus, the dual delayed fluorescence in the MCP-based films played an important role in realizing the slow efficiency roll-offs.

The temperature dependent photophysical properties of doped films A (15 wt% PXZ-CMO:MCP) and B (20 wt% PXZ-CMO:DPEPO) were presented in **Figure 7** and **Tables S3, S4**. Within the temperature region from 78 to 325 K, film A displayed two delayed fluorescence lifetimes at around 1.0 ( $\tau_{d1}$ )  $\mu$ s and 5.0–12.0 ( $\tau_{d2}$ )  $\mu$ s, respectively. The integral ratio of the longer  $\tau_{d2}$  gradually improved upon temperature increasing, suggesting a typical TADF feature (Uoyama et al., 2012; Kaji et al., 2015). For the shorter  $\tau_{d1}$ , the integral ratio displayed slight improvement upon temperature increasing from 78 to 175 K and then obviously decreased upon temperature increasing from 175 to 325 K. Therefore, it is possible that certain conformation transformation mechanism may be included in the emission spectra of film A at high temperature region (above 200 K). In particular, it still exhibited two delayed lifetimes at 77 K, which further suggested the presence of two  $T_1$  excited states of film A (**Table S3**). For film B, the delayed fluorescence was observed when the temperature was improved to 200 K and the delayed lifetime exhibited successive decrease tendency. Therefore, in DPEPO matrix, the triple excited state of PXZ-CMO may be easily quenched and the TADF behavior was only observed at relatively high temperature, which can provide enough energy to promote the RISC process. Thus, for device G1, the existence of dual delayed fluorescence makes it possible to decrease the concentrations of every kind of  $T_1$  excited state and suppress

the TTA processes to realize an extremely low efficiency roll-off in TADF-OLED. In addition, the delayed lifetimes ( $\tau_d$ ) began to decrease when the dopant concentration  $\geq 30$  wt% in both MCP- and DPEPO-based films (**Figure S11**), which could be attributed to that the TTA induced excited state quenching is stronger in the high dopant concentration films. To further verify the molecular structure of PXZ-CMO,  $^1H$  and  $^{13}C$  NMR spectroscopies were measured (**Figures S12, S13**).

## CONCLUSION

In summary, a TADF compound PXZ-CMO featuring a D-A structure was designed and synthesized. The PXZ-CMO:MCP doped films displayed two delayed fluorescence lifetimes at around 1.1 and 9.1  $\mu$ s, respectively. The PXZ-CMO:MCP films were employed as emitting layer to fabricate high performance TADF-OLEDs that exhibited low efficiency roll-offs. The MCP matrix with weak polarity can promote the generation of dual delayed fluorescence for PXZ-CMO molecules. The achievement of dual delayed fluorescence can dilute the concentration of  $T_1$  excited states and suppress the TTA processes in the emitting layer, which is beneficial to the reduction of efficiency roll-off. Therefore, this study provided an efficient approach to achieve the high-efficiency TADF-OLEDs with low efficiency roll-offs.

## AUTHOR CONTRIBUTIONS

YZ, CL, and YW proposed the idea of this manuscript and analyzed the experiment results. YZ and ZL contributed to the synthesis of the materials and the fabrication of the OLEDs. YW wrote the paper.

## FUNDING

This work was supported by the National Basic Research Program of China (2015CB655003), the National Natural Science Foundation of China (91333201 and 51803069), China Postdoctoral Science Foundation (2018M630319 and 2018T110244), Program for JLU Science and Technology Innovative Research Team and Jilin Province-University Program (SXGJSF2017-3).

## SUPPLEMENTARY MATERIAL

The Supplementary Material for this article can be found online at: <https://www.frontiersin.org/articles/10.3389/fchem.2019.00302/full#supplementary-material>

## REFERENCES

- Aydemir, M., Haykir, G., Türksoy, F., Gümüş, S., Dias, F. B., and Monkman, A. P. (2015). Synthesis and investigation of intra-molecular charge transfer state properties of novel donor-acceptor-donor pyridine derivatives: the effects of temperature and environment on molecular configurations and the origin of delayed fluorescence. *Phys. Chem. Chem. Phys.* 17, 25572–25582. doi: 10.1039/C5CP03937A
- Aydemir, M., Xu, S., Chen, C., Bryce, M. R., Chi, Z., and Monkman, A. P. (2017). Photophysics of an asymmetric donor-acceptor-donor TADF molecule and reinterpretation of aggregation-induced TADF emission in these materials. *J. Phys. Chem. C* 121, 17764–17772. doi: 10.1021/acs.jpcc.7b06299
- Cai, M., Song, X., Zhang, D., Qiao, J., and Duan, L. (2017).  $\pi$ - $\pi$  stacking: a strategy to improve the electron mobilities of bipolar hosts for TADF and phosphorescent devices with low efficiency roll-off. *J. Mater. Chem. C* 5, 3372–3381. doi: 10.1039/C7TC00733G

- Chen, J.-X., Liu, W., Zheng, C.-J., Wang, K., Liang, K., Shi, Y.-Z., et al. (2017). Coumarin-Based thermally activated delayed fluorescence emitters with high external quantum efficiency and low efficiency roll-off in the devices. *ACS Appl. Mater. Interfaces* 9, 8848–8854. doi: 10.1021/acsami.6b15816
- Cho, Y. J., Jeon, S. K., and Lee, J. Y. (2016). Molecular engineering of high efficiency and long lifetime blue thermally activated delayed fluorescent emitters for vacuum and solution processed organic light emitting diodes. *Adv. Optical Mater.* 4, 688–693. doi: 10.1002/adom.201500634
- Data, P., Pander, P., Okazaki, M., Takeda, Y., Minakata, S., and Monkman, A. P. (2016). Dibenzo[a,j]phenazine-cores donor-acceptor-donor compounds as green-to-red/NIR thermally activated delayed fluorescence organic light emitters. *Angew. Chem. Int. Ed.* 55, 5739–5744. doi: 10.1002/anie.201600113
- Fu, G. C. (2008). The development of versatile methods for palladium-catalyzed coupling reactions of aryl electrophiles through the use of P(t-Bu)<sub>3</sub> and PCy<sub>3</sub> as ligands. *Acc. Chem. Res.* 41, 1555–1564. doi: 10.1021/ar800148f
- Grabowski, Z. R., Rotkiewicz, K., and Rettig, W. (2003). Structural changes accompanying intramolecular electron transfer: focus on twisted intramolecular charge-transfer states and structures. *Chem. Rev.* 103, 3899–4032. doi: 10.1021/cr940745l
- Guo, Z.-H., Jin, Z.-X., Wang, J.-Y., and Pei, J. (2014). A donor-acceptor-donor conjugated molecule: twist intramolecular charge transfer and piezochromic luminescent properties. *Chem. Commun.* 50, 6088–6090. doi: 10.1039/c3cc48980a
- Hooper, M. W., Utsunomiya, M., and Hartwig, J. F. (2003). Scope and mechanism of palladium-catalyzed amination of five-membered heterocyclic halides. *J. Org. Chem.* 68, 2861–2873. doi: 10.1021/jo0266339
- Huang, J., Nie, H., Zeng, J., Zhuang, Z., Gan, S., Cai, Y., et al. (2017). Highly efficient nondoped OLEDs with negligible efficiency roll-off fabricated from aggregation-induced delayed fluorescence luminogens. *Angew. Chem. Int. Ed.* 56, 12971–12976. doi: 10.1002/anie.201706752
- Kaji, H., Suzuki, H., Fukushima, T., Shizu, K., Suzuki, K., Kubo, S., et al. (2015). Purely organic electroluminescent material realizing 100% conversion from electricity to light. *Nat. Commun.* 6:8476. doi: 10.1038/ncomms9476
- Kim, B. S., and Lee, J. Y. (2014). Phosphine oxide type bipolar host material for high quantum efficiency in thermally activated delayed fluorescent device. *ACS Appl. Mater. Interfaces* 6, 8396–8400. doi: 10.1021/am501301g
- Kim, D.-H., D'Aléo, A., Chen, X.-K., Sandanayaka, A. D. S., Yao, D., Zhao, L., et al. (2018). High-efficiency electroluminescence and amplified spontaneous emission from a thermally activated delayed fluorescent near-infrared emitter. *Nat. Photonics* 12, 98–104. doi: 10.1038/s41566-017-0087-y
- Lee, D. R., Choi, J. M., Lee, C. W., and Lee, J. Y. (2016). Ideal molecular design of blue thermally activated delayed fluorescent emitter for high efficiency, small singlet-triplet energy splitting, low efficiency roll-off, and long lifetime. *ACS Appl. Mater. Interfaces* 8, 23190–23196. doi: 10.1021/acsami.6b05877
- Lee, J., Aizawa, N., and Yasuda, T. (2017). Isobenzofuranone- and chromone-based blue delayed fluorescence emitters with low efficiency roll-off in organic light-emitting diodes. *Chem. Mater.* 29, 8012–8020. doi: 10.1021/acs.chemmater.7b03371
- Lee, S. Y., Yasuda, T., Yang, Y. S., Zhang, Q., and Adachi, C. (2014). Luminous butterflies: efficient exciton harvesting by benzophenone derivatives for full-color delayed fluorescence OLEDs. *Angew. Chem. Int. Ed.* 53, 6402–6406. doi: 10.1002/anie.201402992
- Li, C., Duan, R., Liang, B., Han, G., Wang, S., Ye, K., et al. (2017). Deepred to near-infrared thermally activated delayed fluorescence in organic solid films and electroluminescent devices. *Angew. Chem. Int. Ed.* 56, 11525–11529. doi: 10.1002/anie.201706464
- Li, Y., Li, X.-L., Chen, D., Cai, X., Xie, G., He, Z., et al. (2016). Design strategy of blue and yellow thermally activated delayed fluorescence emitters and their all-fluorescence white OLEDs with external quantum efficiency beyond 20%. *Adv. Funct. Mater.* 26, 6904–6912. doi: 10.1002/adfm.201602507
- Lin, T.-A., Chatterjee, T., Tsai, W.-L., Lee, W.-K., Wu, M.-J., Jiao, M., et al. (2016). Sky-blue organic light emitting diode with 37% external quantum efficiency using thermally activated delayed fluorescence from spiroacridine-triazine hybrid. *Adv. Mater.* 28, 6976–6983. doi: 10.1002/adma.201601675
- Littke, A. F., Schwarz, L., and Fu, G. C. (2002). Pd/P(t-Bu)<sub>3</sub>: a mild and general catalyst for stille reactions of aryl chlorides and aryl bromides. *J. Am. Chem. Soc.* 124, 6343–6348. doi: 10.1021/ja020012f
- Liu, M., Komatsu, R., Cai, X., Sasabe, H., Kamata, T., Nakao, K., et al. (2017). Introduction of twisted backbone: a new strategy to achieve efficient blue fluorescence emitter with delayed emission. *Adv. Optical Mater.* 5:1700334. doi: 10.1002/adom.201700334
- Liu, X.-K., Chen, Z., Zheng, C.-J., Liu, C.-L., Lee, C.-S., Li, F., et al. (2015). Prediction and design of efficient exciplex emitters for high-efficiency, thermally activated delayed-fluorescence organic light-emitting diodes. *Adv. Mater.* 27, 2378–2383. doi: 10.1002/adma.201405062
- Méhes, G., Goushi, K., Potscavage, W. J., and Adachi, C. (2014). Influence of host matrix on thermally-activated delayed fluorescence: effects on emission lifetime, photoluminescence quantum yield, and device performance. *Org. Electron.* 15, 2027–2037. doi: 10.1016/j.orgel.2014.05.027
- Numata, M., Yasuda, T., and Adachi, C. (2015). High efficiency pure blue thermally activated delayed fluorescence molecules having 10H-phenoxaborin and acridan units. *Chem. Commun.* 51, 9443–9446. doi: 10.1039/C5CC00307E
- O'Brien, J. A., Rallabandi, S., Tripathy, U., Paige, M. F., and Steer, R. P. (2009). Efficient S2 state production in ZnTPP-PMMA thin films by triplet-triplet annihilation: Evidence of solute aggregation in photon upconversion systems. *Chem. Phys. Lett.* 475, 220–222. doi: 10.1016/j.cplett.2009.05.039
- Rajamalli, P., Senthilkumar, N., Gandeepan, P., Huang, P.-Y., Huang, M.-J., Ren-Wu, C.-Z., et al. (2016). A new molecular design based on thermally activated delayed fluorescence for highly efficient organic light emitting diodes. *J. Am. Chem. Soc.* 138, 628–634. doi: 10.1021/jacs.5b10950
- Tao, Y., Yuan, K., Chen, T., Xu, P., Li, H., Chen, R., et al. (2014). Thermally activated delayed fluorescence materials towards the breakthrough of organoelectronics. *Adv. Mater.* 26, 7931–7958. doi: 10.1002/adma.201402532
- Uoyama, H., Goushi, K., Shizu, K., Nomura, H., and Adachi, C. (2012). Highly efficient organic light-emitting diodes from delayed fluorescence. *Nature* 492, 234–238. doi: 10.1038/nature11687
- Wang, H., Xie, L., Peng, Q., Meng, L., Wang, Y., Yi, Y., et al. (2014). Novel thermally activated delayed fluorescence materials-thioxanthone derivatives and their applications for highly efficient OLEDs. *Adv. Mater.* 26, 5198–5204. doi: 10.1002/adma.201401393
- Wang, K., Zhao, F., Wang, C., Chen, S., Chen, D., Zhang, H., et al. (2013). High-performance red, green, and blue electroluminescent devices based on blue emitters with small singlet-triplet splitting and ambipolar transport property. *Adv. Funct. Mater.* 23, 2672–2680. doi: 10.1002/adfm.201202981
- Wang, K., Zheng, C.-J., Liu, W., Liang, K., Shi, Y.-Z., Tao, S.-L., et al. (2017). Avoiding energy loss on TADF emitters: controlling the dual conformations of D-A structure molecules based on the pseudoplanar segments. *Adv. Mater.* 29:1701476. doi: 10.1002/adma.201701476
- Wang, S., Yan, X., Cheng, Z., Zhang, H., Liu, Y., and Wang, Y. (2015). Highly efficient near-infrared delayed fluorescence organic light emitting diodes using a phenanthrene-based charge-transfer compound. *Angew. Chem. Int. Ed.* 54, 13068–13072. doi: 10.1002/anie.201506687
- Wei, X., Chen, Y., Duan, R., Liu, J., Wang, R., Liu, Y., et al. (2017). Triplet decay-induced negative temperature dependence of the transient photoluminescence decay of thermally activated delayed fluorescence emitter. *J. Mater. Chem. C* 5, 12077–12084. doi: 10.1039/C7TC04025C
- Wolfe, J. P., Wagaw, S., Marcoux, J.-F., and Buchwald, S. L. (1998). Rational development of practical catalysts for aromatic carbon-nitrogen bond formation. *Acc. Chem. Res.* 31, 805–818. doi: 10.1021/ar9600650
- Wu, T.-L., Huang, M.-J., Lin, C.-C., Huang, P.-Y., Chou, T.-Y., Chen-Cheng, R.-W., et al. (2018). Diboron compound-based organic light-emitting diodes with high efficiency and reduced efficiency roll-off. *Nat. Photonics* 12, 235–240. doi: 10.1038/s41566-018-0112-9
- Yang, Z., Mao, Z., Xie, Z., Zhang, Y., Liu, S., Zhao, J., et al. (2017). Recent advances in organic thermally activated delayed fluorescence materials. *Chem. Soc. Rev.* 46, 915–1016. doi: 10.1039/C6CS00368K
- Yu, L., Wu, Z., Zhong, C., Xie, G., Zhu, Z., Ma, D., et al. (2017). Pure organic emitter with simultaneous thermally activated delayed fluorescence and room-temperature phosphorescence: thermal-controlled triplet recycling channels. *Adv. Optical Mater.* 5:1700588. doi: 10.1002/adom.201700588
- Zeng, W., Lai, H.-Y., Lee, W.-K., Jiao, M., Shiu, Y.-J., Zhong, C., et al. (2018). Achieving nearly 30% external quantum efficiency for orange-red organic light emitting diodes by employing thermally activated delayed fluorescence emitters

- composed of 1,8-naphthalimide-acridine hybrids. *Adv. Mater.* 30:1704961. doi: 10.1002/adma.201704961
- Zhang, D., Duan, L., Li, C., Li, Y., Li, H., Zhang, D., et al. (2014a). High-efficiency fluorescent organic light-emitting devices using sensitizing hosts with a small singlet–triplet exchange energy. *Adv. Mater.* 26, 5050–5055. doi: 10.1002/adma.201401476
- Zhang, J., Duan, C., Han, C., Yang, H., Wei, Y., and Xu, H. (2016a). Balanced dual emissions from tridentate phosphine-coordinate copper(i) complexes toward highly efficient yellow OLEDs. *Adv. Mater.* 28, 5975–5979. doi: 10.1002/adma.201600487
- Zhang, Q., Kuwabara, H., Potsavage, W. J., Huang, S., Hatae, Y., Shibata, T., et al. (2014b). Anthraquinone-based intramolecular charge-transfer compounds: computational molecular design, thermally activated delayed fluorescence, and highly efficient red electroluminescence. *J. Am. Chem. Soc.* 136, 18070–18081. doi: 10.1021/ja510144h
- Zhang, Q., Li, B., Huang, S., Nomura, H., Tanaka, H., and Adachi, C. (2014c). Efficient blue organic light-emitting diodes employing thermally activated delayed fluorescence. *Nat. Photonics* 8, 326–332. doi: 10.1038/nphoton.2014.12
- Zhang, Q., Li, J., Shizu, K., Huang, S., Hirata, S., Miyazaki, H., et al. (2012). Design of efficient thermally activated delayed fluorescence materials for pure blue organic light emitting diodes. *J. Am. Chem. Soc.* 134, 14706–14709. doi: 10.1021/ja306538w
- Zhang, Y., Ma, H., Wang, S., Li, Z., Ye, K., Zhang, J., et al. (2016b). Supramolecular structure-dependent thermally-activated delayed fluorescence (TADF) properties of organic polymorphs. *J. Phys. Chem. C*, 120, 19759–19767. doi: 10.1021/acs.jpcc.6b05537
- Zhang, Y., Miao, Y., Song, X., Gao, Y., Zhang, Z., Ye, K., et al. (2017). Single-molecule-based white-light emissive organic solids with molecular-packing-dependent thermally activated delayed fluorescence. *J. Phys. Chem. Lett.* 8, 4808–4813. doi: 10.1021/acs.jpcl.7b02213

**Conflict of Interest Statement:** The authors declare that the research was conducted in the absence of any commercial or financial relationships that could be construed as a potential conflict of interest.

Copyright © 2019 Zhang, Li, Li and Wang. This is an open-access article distributed under the terms of the Creative Commons Attribution License (CC BY). The use, distribution or reproduction in other forums is permitted, provided the original author(s) and the copyright owner(s) are credited and that the original publication in this journal is cited, in accordance with accepted academic practice. No use, distribution or reproduction is permitted which does not comply with these terms.